Turkish Journal of Electrical Engineering & Computer Sciences

http://journals.tubitak.gov.tr/elektrik/

Research Article

Turk J Elec Eng & Comp Sci
(2018) 26: 2234 – 2245

doi:10.3906/elk-1803-76

A low-complexity RARE-based 2-D DOA estimation algorithm for a mixture of circular and strictly noncircular sources

Kashif SHABIR, Tarek HASAN AL MAHMUD, Rui ZHENG, Zhongfu YE*
Department of Electronic Engineering and Information Science, University of Science and Technology of China, Hefei, P.R. China

Received: 12.03.2018 • **Accepted/Published Online:** 05.08.2018 • **Final Version:** 28.09.2018

Abstract: A new rank reduction (RARE)-based two-dimensional (2-D) direction of arrival (DOA) estimation algorithm is proposed considering a mixture of circular and strictly noncircular sources. To enhance array aperture, a geometry of three uniform linear arrays is considered and then treated as displaced arrays from a virtual array using a simple linear transformation. The received data and the conjugated counterpart are combined together, exploiting the noncircular property. Both sources can be estimated separately by designing and exploiting the distinctive nature of circular and noncircular steering vectors. However, a 2-D spectrum search would lead to a high computational complexity burden. To reduce this high computational complexity burden, a novel RARE-based method is proposed, which plays a vital role by decomposing 2-D observation space into two successive 1-D peak search functions. The proposed method has some distinctive advantages: it can enhance the array aperture utilization, it can provide better estimation accuracy when mixed sources are greater than the number of sensors, it can estimate a larger number of mixed sources than the number of sensors, and finally it can automatically pair 2-D DOAs without any complicated pairing formulation. Extensive simulation results are provided to demonstrate the effectiveness of the proposed method.

Key words: Rank reduction, two-dimensional, direction of arrival, circular and strictly noncircular sources, uniform linear arrays, underdetermined, array aperture utilization

1. Introduction

Direction of arrival (DOA) estimation in array signal processing is very important in order to pinpoint the sources precisely. Accurate estimation of DOA is an indispensable part of many real-world applications like radar, microphone array systems, sonar, and speech processing. Over the decades, a number of sophisticated techniques have been developed like well-known multiple signal classification (MUSIC) [1, 2], estimation of signal parameters via rotational invariance technique (ESPRIT) [3], and their variant algorithms[4–6]. These techniques are known as subspace (SS) techniques. In past literature, the focus was to exploit the signal's spatial properties to solve DOA estimation problems. However, recently other properties have also been exploited to solve this problem, like the noncircular property as in [7]. These types of properties not only enhance the estimation accuracy but also give us an opportunity to resolve more sources than sensors. Hence, such types of estimators are very helpful in wireless communications. Many methods have been proposed considering different array geometries, like two-parallel uniform linear arrays (ULAs). In [8], Xia et al. proposed

*Correspondence: yezf@ustc.edu.cn

decoupling of 2-D into two successive 1-D MUSIC techniques to estimate noncircular sources considering two parallel ULAs. L-shaped ULAs [9] and ESPRIT-based DOA estimation [10, 11] were also explored. In [12], a MUSIC-like estimation was developed for noncircular sources. whereas in [13] a 2-D based DOA estimation of noncircular sources was designed using the simultaneous SVD technique. In [14], a joint elevation and azimuth direction-finding algorithm was proposed considering an L-shaped array to remove pairing problems. A more complex and real problem arises in real-time communications when there is a mixture of circular and noncircular signals impinging on the array at once, like in adaptive modulation where one terminal transmits circular signals (quadrature phase shift keying) and the other transmits noncircular signals (binary phase shift keying) simultaneously. Several 2-D DOA estimation methods have been proposed to solve this problem. In [15] an improved MUSIC-based algorithm was designed to estimate circular and noncircular sources exploiting the noncircular property. However, its performance degraded severely when angle separation was small and it could not discriminate both types of sources when DOAs of both sources coincided. In particular, in [16] the authors developed a joint diagonalization 2-D method to estimate DOAs for a mixture of circular and strictly noncircular sources, considering a uniform rectangular array (URA). In [17], a new reduced rank-based method was designed considering three parallel ULAs considering only circular sources. In [18] an improved algorithm was proposed which estimates both types of DOAs individually by exploiting differences between the noncircular properties of signals. A sparse (ERARE)-based DOA estimation algorithm was designed in [19] to estimate both sources separately. However, a rank reduction-based 2-D DOA estimation for a mixture of circular and strictly noncircular sources considering three parallel ULAs has not been considered yet in the literature. The remaining paper will be divided as follows: Section 2 will provide a basic structure of three parallel ULAs along with signal model. The proposed method will be developed in Section 3 and then RARE-based DOA estimation of both sources will be obtained separately after applying the MUSIC technique. Section 4 will provide extensive simulation results to show the performance of our proposed method.

1.1. Symbols and abbreviations

We use lowercase (uppercase) bold characters to denote vectors (matrices). In particular, $(.)^*$ implies complex conjugation, whereas $(.)^T$ and $(.)^H$ respectively denote the transpose and conjugate transpose of a matrix or vector, $diag\,(.)$ denotes a diagonal matrix, and $\mathrm{E}\,(.)$ is the statistical expectation operator.

2. Data model

Consider an array geometry consisting of three parallel ULAs placed along the x-y plane as shown in Figure 1. Each subarray consists of M sensors and hence the total number of sensors is $M' = 3M$. Interspacing between each sensor and each ULA is considered as half wavelength. Consider K (previously known) uncorrelated, narrow-band, 2-D, far-field sources impinging on this geometry, with angles θ_k and φ_k $k = 1, 2, ..., K$. Furthermore, these K sources are considered as a mixture of two types of sources: circular K_c and strictly noncircular K_n sources such that $K = K_n + K_c$. A signal is circular if its second-order elliptic covariance is $\mathrm{E}[ss] = 0$; otherwise, it is noncircular. Therefore, the output at each subarray at the tth snapshot can be written as

$$\begin{aligned}
\mathbf{x}_1(t) &= \mathbf{A}\mathbf{s}(t) + \mathbf{w}_1(t), \\
\mathbf{x}_2(t) &= \mathbf{A}_{\ 2}\,\mathbf{s}(t) + \mathbf{w}_2(t), \\
\mathbf{x}_3(t) &= \mathbf{A}_{\ 3}\,\mathbf{s}(t) + \mathbf{w}_3(t),
\end{aligned} \tag{1}$$

where $\mathbf{A} = [\mathbf{a}(\theta_1, \varphi_1), ..., \mathbf{a}(\theta_{K_n}, \varphi_{K_n}), \mathbf{a}(\theta_{K_n+1}, \varphi_{K_n+1}, ..., \mathbf{a}(\theta_K, \varphi_K)]$ is a mixed steering matrix with steering

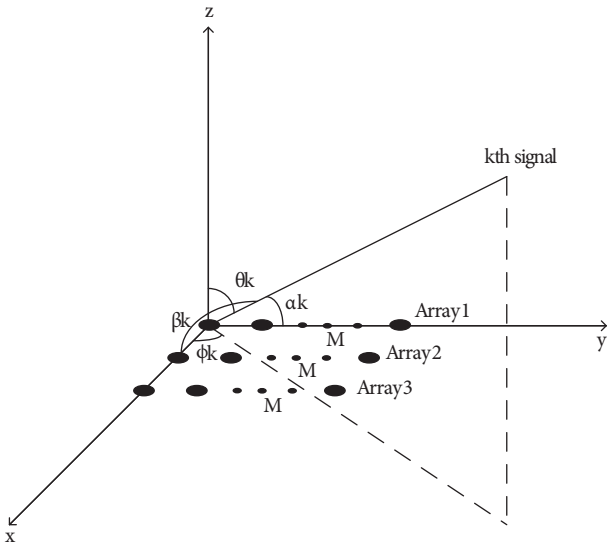

Figure 1. Geometry of three planar parallel ULAs.

vector $\mathbf{a}(\theta_k, \varphi_k) = \left[1, ..., e^{j\frac{2\pi d}{\lambda}(M-1)\sin\theta_k \sin\varphi_k}\right]^T$. Similarly, $_2 = diag\left[e^{j\frac{2\pi d}{\lambda}\sin\theta_1 \sin\varphi_1}, ..., e^{j\frac{2\pi d}{\lambda}\sin\theta_K \sin\varphi_K}\right]$, $_3 = diag\left[e^{j\frac{4\pi d}{\lambda}\sin\theta_1 \sin\varphi_1}, ..., e^{j\frac{2\pi d}{\lambda}\sin\theta_K \sin\varphi_K}\right]$, and $\mathbf{s}(t) = [b_1 s_1(t), ..., b_k s_{K_n}(t), s_{K_n+1}(t), ..., s_K(t)]^T$ are the steering element matrices and the transmitted mixture of circular signals vector and strictly noncircular signals vector with $b_k = \eta_k e^{j\phi_k}$ having kth source noncircularity rate and phase shift, respectively. The circularity rate actually defines the type of signal, like $\eta = 0$ means a circular signal and similarly $0 < \eta \leq 1$ means the signal is noncircular with a special case when $\eta = 1$ represents a strictly noncircular signal. Similarly, noise vectors $\mathbf{w}_1(t), \mathbf{w}_2(t)$, and $\mathbf{w}_3(t)$ are considered Gaussian and circular with zero mean and σ^2 variance, respectively.

3. Proposed method

In this section, the 2-D DOA estimation algorithm will be described in detail considering a mixture of circular and strictly noncircular sources exploiting the noncircular property by stacking original data with the conjugated part. First, the data can be concatenated as

$$\mathbf{z}(t) = \begin{bmatrix} \mathbf{x}_1(t) \\ \mathbf{x}_2(t) \\ \mathbf{x}_3(t) \end{bmatrix} = \begin{bmatrix} \mathbf{A} \\ \mathbf{A}\ _2 \\ \mathbf{A}\ _3 \end{bmatrix} \mathbf{s}(t) + \begin{bmatrix} \mathbf{w}_1(t) \\ \mathbf{w}_2(t) \\ \mathbf{w}_3(t) \end{bmatrix} \tag{2}$$

$$= \mathbf{C}\mathbf{s}(t) + \mathbf{w}(t), \tag{3}$$

where $\mathbf{C} = \begin{bmatrix} \mathbf{A}^T & (\mathbf{A}\ _2)^T & (\mathbf{A}\ _3)^T \end{bmatrix}^T \in C^{M' \times K}$, $\mathbf{s}(t) \in C^{K \times 1}$, and $\mathbf{w}(t) \in C^{M' \times 1}$. $\mathbf{C}$ is the extended steering matrix consisting of K_c circular and K_n noncircular number of column vectors. Hence, $\mathbf{C}$ can be represented as

$$\mathbf{C} = \begin{bmatrix} \mathbf{C}_n & \mathbf{C}_c \end{bmatrix} \in C^{M' \times (K_n + K_c.)} \tag{4}$$

The three parallel ULAs can be translated along the y-axis in such a way that they give us M' longer virtual elements [20]. In order to achieve a longer displaced array, consider $\cos\alpha_k = \sin\theta_k \sin\varphi_k, \alpha_k \in [0,\pi]$ and $\cos\beta_k = \sin\theta_k \cos\varphi_k, \beta_k \in [0,\pi]$. Then the steering vector of the longer virtual array can be expressed as $\mathbf{c}(\alpha_k) = \left[1, ..., e^{j\frac{2\pi d}{\lambda}(3M-1)\cos\alpha_k}\right] \in C^{M'\times 1}$. Hence, the relationship between translated and nontranslated steering vectors can be written as

$$\mathbf{c}(\alpha_k, \beta_k) = \mathbf{c}(\theta_k, \varphi_k) = diag\left[\mathbf{c}(\alpha_k)\right] \mathbf{Tq}(\alpha_k, \beta_k,) \tag{5}$$

$$\mathbf{T} = \begin{bmatrix} \mathbf{1}_{1\times M} & \mathbf{0}_{1\times M} & \mathbf{0}_{1\times M} \\ \mathbf{0}_{1\times M} & \mathbf{1}_{1\times M} & \mathbf{0}_{1\times M} \\ \mathbf{0}_{1\times M} & \mathbf{0}_{1\times M} & \mathbf{1}_{1\times M} \end{bmatrix}^T, \tag{6}$$

where $\mathbf{q}(\alpha_k, \beta_k) = \left[1, e^{-j\frac{2\pi dM}{\lambda}\cos\alpha_k} e^{j\frac{4\pi d}{\lambda}\cos\beta_k}, e^{-j\frac{2\pi d(2M)}{\lambda}\cos\alpha_k} e^{j\frac{4\pi d}{\lambda}\cos\beta_k}\right]^T \in C^{3\times 1}$ represents a phase shift vector. Then, considering the noncircular property, a translated extended data vector can be designed by stacking original data and the conjugated counterpart as

$$\widehat{\mathbf{z}} = \begin{bmatrix} \mathbf{z} \\ \mathbf{z}^* \end{bmatrix} = \begin{bmatrix} \mathbf{Cs} \\ \mathbf{C}^* \mathbf{s}^* \end{bmatrix} + \begin{bmatrix} \mathbf{w} \\ \mathbf{w}^* \end{bmatrix} = \widehat{\mathbf{C}}\widehat{\mathbf{s}} + \widehat{\mathbf{w}}, \tag{7}$$

$$\widehat{\mathbf{C}} = [\widehat{\mathbf{c}}_{n,1}, ..., \widehat{\mathbf{c}}_{n,K_n}, \widehat{\mathbf{c}}_{c,1}, ..., \widehat{\mathbf{c}}_{n,K_c}]. \tag{8}$$

After putting Eq. (5) into Eq. (8), we can get

$$\widehat{\mathbf{c}}_{n,k} = \begin{bmatrix} b_{n,k}\,\mathbf{c}(\alpha_k, \beta_k) \\ {b_{n,k}}^*\,\mathbf{c}(\alpha_k, \beta_k)^* \end{bmatrix} \in C^{2M'\times 1}, k = 1, ..., K_n, \tag{9}$$

and similarly

$$\widehat{\mathbf{C}}_{c,k} = \begin{bmatrix} \mathbf{c}(\alpha_k, \beta_k) & \mathbf{0}_{M'\times 1} \\ \mathbf{0}_{M'\times 1} & \mathbf{c}(\alpha_k, \beta_k)^* \end{bmatrix} \in C^{2(M'\times 1)}, k = 1, ..., K_c \tag{10}$$

with

$$\widehat{\mathbf{s}} = [\mathbf{s}_{n,1}, ..., \mathbf{s}_{n,K_n}, \mathbf{s}_{c,1}, {\mathbf{s}_{c,1}}^*, ..., \mathbf{s}_{c,K_c}, {\mathbf{s}_{c,K_c}}^*] \in C^{K'\times 1} \tag{11}$$

is a $K'\times 1$ vector at the kth snapshot, where $K' = K_n + K_c$ Hence, the covariance matrix of $\widehat{\mathbf{z}}$ can be expressed as

$$\widehat{\mathbf{w}} = \begin{bmatrix} \mathbf{w} \\ \mathbf{w}^* \end{bmatrix} \in C^{2M'\times 1}, \tag{12}$$

$$\mathbf{R} = \mathrm{E}\left[\widehat{\mathbf{z}}\widehat{\mathbf{z}}^H\right] = \widehat{\mathbf{C}}\,\mathbf{R}_s\,\widehat{\mathbf{C}}^H + \sigma_n^2\,\mathbf{I}_{2M'}, \tag{13}$$

where $\mathbf{R}_s$ is the source covariance matrix for $\widehat{\mathbf{s}}$. However, practically we only have finite samples of observed data. Therefore, practically the covariance matrix can be written as

$$\widehat{\mathbf{R}} \cong \mathbf{E}_s\ {}_s\ {\mathbf{E}_s}^H + \mathbf{E}_n\ {}_n\ {\mathbf{E}_n}^H. \tag{14}$$

Exploiting the orthogonality between $\mathbf{E}_n$ and $\widehat{\mathbf{C}}$, we can design estimators to estimate 2-D DOAs for both types of sources separately using the rank reduction method.

3.1. 2-D DOA estimation of strictly noncircular sources

Since noise subspace and signal subspace are orthogonal to each other, exploiting this orthogonality we can design an estimator that can be used to estimate noncircular sources. Since

$$\mathbf{E}_n{}^H \widehat{\mathbf{c}}_{n,k} = 0, \tag{15}$$

instead of estimating the 2-D spectrum search, we can divide the 2-D search into two 1-D search functions using the RARE method [20] to reduce complexity.

$$\mathbf{E}_n{}^H \begin{bmatrix} b_{n,k}\,\mathbf{c}\left(\alpha_k,\beta_k\right) \\ b_{n,k}{}^*\,\mathbf{c}\left(\alpha_k,\beta_k\right)^* \end{bmatrix} = \mathbf{E}_n{}^H \begin{bmatrix} b_{n,k}\left\{diag\left[\mathbf{c}\left(\alpha_k\right)\right]\mathbf{Tq}\left(\alpha_k,\beta_k\right)\right\} \\ b_{n,k}{}^*\left\{diag\left[\mathbf{c}\left(\alpha_k\right)\right]\mathbf{Tq}\left(\alpha_k,\beta_k\right)\right\}^* \end{bmatrix},$$

$$\mathbf{E}_n{}^H \begin{bmatrix} diag\left[\mathbf{c}\left(\alpha_k\right)\right]\mathbf{Tq} \\ diag\left[\mathbf{c}\left(\alpha_k\right)^*\right]\mathbf{T}^*\,\mathbf{q}^* \end{bmatrix} \begin{bmatrix} b_{n,k} \\ b_{n,k}{}^* \end{bmatrix} = 0,$$

$$\begin{bmatrix} diag\left[\mathbf{c}\left(\alpha_k\right)\right] & \mathbf{0} \\ \mathbf{0} & diag\left[\mathbf{c}\left(\alpha_k\right)^*\right] \end{bmatrix} \begin{bmatrix} \mathbf{q} & \mathbf{0} \\ \mathbf{0} & \mathbf{q}^* \end{bmatrix} \begin{bmatrix} \mathbf{T} & \mathbf{0} \\ \mathbf{0} & \mathbf{T}^* \end{bmatrix} \begin{bmatrix} b_{n,k} \\ b_{n,k}{}^* \end{bmatrix} = \mathbf{c}_{ext}\,T_{ext}\,\mathbf{Q}_{ext}\,\mathbf{b'}_{n,k}, \tag{16}$$

where $\mathbf{c}_{ext} = blkdiag\left[diag\left[\mathbf{c}\left(\alpha_k\right)\right], diag\left[\mathbf{c}\left(\alpha_k\right)^*\right]\right] \in C^{2\left(M'\times 3\right)}, \mathbf{Q}_{ext} = blkdiag\left[\mathbf{q},\mathbf{q}^*\right] \in C^{6\times 2}$, $\mathbf{T}_{ext} = blkdiag\left[\mathbf{T},\mathbf{T}^*\right] \in C^{2\left(M'\times 3\right)}$, and $\mathbf{b'}_{n,k} = \begin{bmatrix} b_{n,k} \\ b_{n,k}{}^* \end{bmatrix} \in C^{2\times 1}$. Now the MUSIC cost function for noncircular sources can be designed as

$$f_n\left(\alpha_k,\beta_k\right) = \mathbf{Q}_{ext}{}^H\,\mathbf{T}_{ext}{}^H\,\mathbf{c}_{ext}{}^H\;\mathbf{E}_n{}^H\,\mathbf{E}_n\,\mathbf{c}_{ext}\,\mathbf{T}_{ext}\,\mathbf{Q}_{ext}$$

$$= \mathbf{Q}_{ext}{}^H\,\mathbf{B}_n\left(\alpha_k\right)\mathbf{Q}_{ext}, \tag{17}$$

where $\mathbf{B}_n\left(\alpha_k\right) = \mathbf{T}_{ext}{}^H\,\mathbf{c}_{ext}{}^H\,\mathrm{E}_n{}^H\,\mathbf{E}_n\,\mathbf{c}_{ext}\,\mathbf{T}_{ext}$ only contains information of parameter $\alpha_k, k = 1,...,K$. Hence, we have separated 2-D DOAs into two consecutive 1-D parts. Therefore, the MUSIC cost function to calculate α_k can be designed as

$$f_n\left(\alpha_k\right) = \frac{1}{\det\left\{\mathbf{B}_n\left(\alpha_k\right)\right\}}. \tag{18}$$

$f_n\left(\alpha_k\right)$ equals zero only when $\mathbf{B}_n\left(\alpha_k\right)$ drops rank means acting as reduced rank. Hence, using the above equation, the K largest peaks can be found for $k = 1,...,K$. After that, values of β_k can be estimated using the RARE technique having prior knowledge of $\breve{\alpha}_k$s as

$$f_n\left(\beta_k\right) = \frac{1}{\det\left\{\mathbf{Q}_{ext}{}^H\,\mathbf{B}_n\left(\breve{\alpha}_k\right)\mathbf{Q}_{ext}.\right\}} \tag{19}$$

3.2. 2-D DOA estimation of circular sources

Similarly, circular sources can also be estimated exploiting the orthogonality between $\widehat{\mathbf{C}}_{c,k}$ and $\mathbf{E}_n$ as

$$\mathbf{E}_n{}^H\,\widehat{\mathbf{C}}_{c,k} = \mathbf{E}_n{}^H \begin{bmatrix} \mathbf{c}\left(\alpha_k,\beta_k\right) & \mathbf{0}_{M'\times 1} \\ \mathbf{0}_{M'\times 1} & \mathbf{c}\left(\alpha_k,\beta_k\right)^* \end{bmatrix} = 0. \tag{20}$$

Similarly, it can be deduced from Eq. (21) that

$$\mathbf{E}_n{}^H \begin{bmatrix} \mathbf{c}(\alpha_k, \beta_k) \\ \mathbf{0}_{M' \times 1} \end{bmatrix} = 0 \tag{21}$$

and

$$\mathbf{E}_n{}^H \begin{bmatrix} \mathbf{0}_{M' \times 1} \\ \mathbf{c}(\alpha_k, \beta_k)^* \end{bmatrix} = 0. \tag{22}$$

Furthermore, $\mathbf{E}_n$ can be partitioned into two equally sized submatrices like $\mathbf{E}_n = \left[\mathbf{E}_{n1}{}^T, \mathbf{E}_{n2}{}^T\right]^T$.
Hence,

$$\mathbf{c}(\alpha_k, \beta_k)^H \mathbf{E}_{n1} \mathbf{E}_{n1}{}^H \mathbf{c}(\alpha_k, \beta_k) = 0, \tag{23}$$

$$\mathbf{c}(\alpha_k, \beta_k)^T \mathbf{E}_{n2} \mathbf{E}_{n2}{}^H \mathbf{c}(\alpha_k, \beta_k)^* = 0. \tag{24}$$

It can be easily shown that Eqs. (23) and (24) both are equal, as shown in the Appendix.
Since

$$\mathbf{c}(\alpha_k, \beta_k) = diag[\mathbf{c}(\alpha_k)] \mathbf{Tq}(\alpha_k, \beta_k), \tag{25}$$

then

$$[diag[\mathbf{c}(\alpha_k)] \mathbf{Tq}(\alpha_k, \beta_k)]^H \mathbf{E}_{n1} \mathbf{E}_{n1}{}^H diag[\mathbf{c}(\alpha_k)] \mathbf{Tq}(\alpha_k, \beta_k) = 0, \tag{26}$$

$$\mathbf{q}^H \mathbf{T}^H diag[\mathbf{c}(\alpha_k)]^H \mathbf{E}_{n1} \mathbf{E}_{n1}{}^H diag[\mathbf{c}(\alpha_k)] \mathbf{Tq} = 0, \tag{27}$$

$$\mathbf{q}^H \mathbf{B}_c(\alpha_k) \mathbf{q} = 0, \tag{28}$$

where $\mathbf{B}_c(\alpha_k) = diag[\mathbf{c}(\alpha_k)]^H \mathbf{E}_{n1} \mathbf{E}_{n1}{}^H diag[\mathbf{c}(\alpha_k)]$ only contains information (circular sources) of $\alpha_k, k = 1, ..., K_c$. Therefore, the MUSIC cost function can be designed to calculate α_k as

$$f_c(\alpha_k) = \frac{1}{\det\{\mathbf{B}_c(\alpha_k).\}} \tag{29}$$

$f_c(\alpha_k)$ equals zero only when $\mathbf{B}_c(\alpha_k))$ drops rank means acting as reduced rank. Hence, using the above equation, the K_c largest peaks can be found for $k = 1, ..., K_c$. Similarly, values of β_k can also be estimated using the RARE technique having prior knowledge of $\hat{\alpha}_k$s as

$$f_c(\beta_k) = \frac{1}{\det\{\mathbf{q}^H \mathbf{B}_c(\hat{\alpha}_k) \mathbf{q}.\}} \tag{30}$$

The relationship between α_k, β_k and θ_k, φ_k can be defined using $\aleph_k = \cos\beta_k + j\cos\alpha_k$. From this, estimated 2-D angles can be calculated as

$$\hat{\theta}_k = angle(\aleph_k), \tag{31}$$

$$\hat{\varphi}_k = \sin^{-1}(amp(\aleph_k)). \tag{32}$$

Note that estimators in Eqs. (18) and (19) estimate 2-D DOAs of both circular and noncircular sources, whereas estimators in Eqs. (29) and (30) only estimate 2-D DOAs of circular sources. Hence, using information from

Eqs. (18) and (19) and from Eqs. (29) and (30), one can identify each type of source separately from a mixture of incident signals. One of the important observations is that both estimators in Eqs. (19) and (30) are also designed based on the RARE principle; however, the difference is mainly the design of noise subspace. In the latter, noise subspace is half that compared to the former. A summary of the proposed algorithm is provided in the Table.

Table. Summary of the proposed algorithm.

Given: $\widehat{\mathbf{R}}$, K_c, K_n, $\mathbf{T}$, $\mathbf{T}_{ext}$, $\mathbf{q}$, and $\mathbf{Q}_{ext}$.
Output: $\hat{\theta}$ and $\hat{\varphi}$.
Step 1. Design an extended received vector using Eq. (7) exploiting noncircularity.
Step 2. Design covariance matrix $\widehat{\mathbf{R}}$ from step 1.
Step 3. Perform EVD on $\widehat{\mathbf{R}}$ and get noise subspace $\mathbf{E}_n$.
Step 4. Use Eqs. (18) and (19) to estimate α and β to estimate K number of sources.
Step 5. Get $\mathbf{E}_{n1}$ from $\mathbf{E}_n$.
Step 6. Use Eqs. (29) and (30) to estimate only K_c circular sources.
Step 7. Identify 2-D angles of only noncircular sources using step 4 and step 6.
Step 8. Finally get original estimated $\hat{\theta}$ and $\hat{\varphi}$ of both sources with the help of Eqs. (31) and (32).

Remark 1 If the incident signals are all noncircular, the proposed method is converted into Liu's [21] method and performance of the proposed method will also become similar to Liu's method.

Remark 2 Here we will give a computational complexity analysis of the proposed method in term of complex multiplications. This complexity can be divided into three parts: construction complexity of $\widehat{\mathbf{R}}$, EVD complexity of $\widehat{\mathbf{R}}$, and spectral searching complexity. The construction complexity of $\widehat{\mathbf{R}}$ is $O\left((2M')^2 L\right)$. The EVD complexity is $O\left((2M')^3\right)$ and the spectral search complexity can be written in terms of several 1-D spatial spectrum searches as our proposed method decomposes the 2-D spectral search into several 1-D search functions. Hence, the total spatial spectrum search complexity is $O\left(\frac{\pi}{\theta}(2M')^2 + K\frac{\pi}{\varphi}(2M')^2 + \frac{\pi}{\theta}(M')^2 + K_c\frac{\pi}{\varphi}(M')^2\right)$.

Remark 3 : Decomposing 2-D DOAs into several 1-D DOAs provides another benefit: it can automatically pair 2-D DOAs without any additional complexity. Hence, there is no additional complexity needed to pair 2-D DOAs.

Remark 4 : The proposed method can estimate a larger number of sources as compared to the number of sensors and it can also provide better estimation accuracy under the limit of high-resolution methods.

Remark 5 : Xia's method can estimate $K_n + K_c = 2(M-1)$ sources, whereas our proposed method can estimate $K_n + 2K_c = 6(M-1)$ and Liu's method can estimate only $K_n = 6(M-1)$ sources, respectively. Hence, overall, our method can estimate more mixed sources as compared to Xia's and Liu's methods.

4. Simulation results

In this section, the performance of the proposed method is validated by various simulations. In all enumerated simulations, the number of sensors in our proposed method and Xia's method are equal to twelve in such a way that in our proposed method each subarray consist of four sensors, whereas in Xia's method each subarray consist of six sensors. All circular ($\eta = 0$) and strictly noncircular ($\eta = 1$) signals are considered to have equal

power. However, this algorithm is equally applicable for any arbitrary noncircular source. BPSK signals ($\eta = 1$) are generated as noncircular signals and QPSK signals ($\eta = 0$) are generated as circular signals. The SNR can be defined as $10\log_{10}\left({\sigma_s}^2/{\sigma_n}^2\right)$, where ${\sigma_s}^2$ and ${\sigma_n}^2$ are the signal and noise covariance, respectively. Root mean square error ($RMSE$) is used as a performance measuring tool to calculate estimation performance of different methods considered in this paper, defined as

$$RMSE = \sqrt{\sum_{k=1}^{K}\sum_{m=1}^{MC}\left[\left(\bar{\nu}_{k,m} - \nu_{k,m}\right)^2\right]}, \tag{33}$$

where K is the number of the mixture of circular and noncircular sources, MC stands for Monte Carlo simulations, $\bar{\nu}_{k,m}$ is the estimated DOA of either θ or φ, and $\nu_{k,m}$ represents the original 2-D angles. Xia's and Liu's methods are considered for a comparison with our proposed method.

4.1. RMSE performance against SNR

In this simulation, our objective is to show the RMSE performance of the proposed method and compare it with Xia's previously proposed method. In order to show the effectiveness of the proposed method we consider five uncorrelated signals coming from directions (54.52,37.87), (22.55,26.91), (45.0,10.0), (11.20,–63.34), and (38.99,–114.28). Furthermore, we consider three cases where case I, case II, and case III contain one, two, and three BPSK signals and the rest of them are QPSK sources, respectively. The number of snapshots is 1000, averaged over 200 MC simulations with SNR changing from 0 dB to 30 dB. Figures **??**a and 2b show the RMSE performance of the proposed method along with Xia's method considering different cases. The proposed method outperforms Xia's method in all cases, especially in case III, where our method completely outperform Xia's method in terms of both the estimated angles. One of the important observations is that the performance of the proposed method starts improving from case I to case III, since the noise subspace dimension increases as the number of BPSK signals increases.

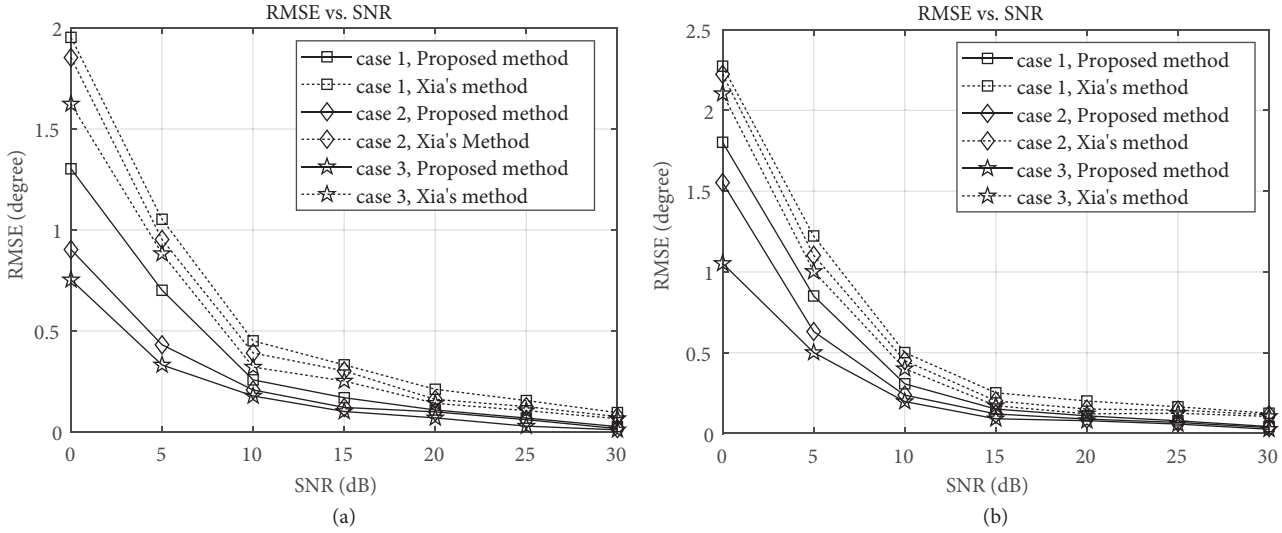

Figure 2. RMSE versus SNR at 1000 snapshots: (a) θ (b) φ.

4.2. RMSE performance against angle separation

The sole objective of this simulation is to show the performance of the proposed method considering different angle separations. The angle separation Δ is varying from 5 to 25 degrees. The number of snapshots is 1200 while fixing SNR at 20 dB. Four uncorrelated 2-D sources having DOAs from directions (61.03, 28.88), ((61.03+Δ),(28.88+Δ)), (18.16,–33.85), and ((18.16+Δ), (–33.85+Δ)) are impinging on the proposed array. Additionally, to show the efficient effectiveness of the proposed method, these sources are distributed into different cases like case I, case II, and case III where one, two, and three BPSK signals are present and the remaining sources are QPSK sources alternatively. Again, our proposed method outperforms Xia's method in all cases as shown in Figures 3a and 3b, especially in case III, and its performance increases with the angle separation, which is an obvious factor. One of the important observations is that our proposed method in case III not only outperforms Xia's method in terms of all three cases but our method's RMSE performance is better as compared to previous case I and case II. This shows that with the increase of BPSK (noncircular) sources the overall performance of the system is also improved.

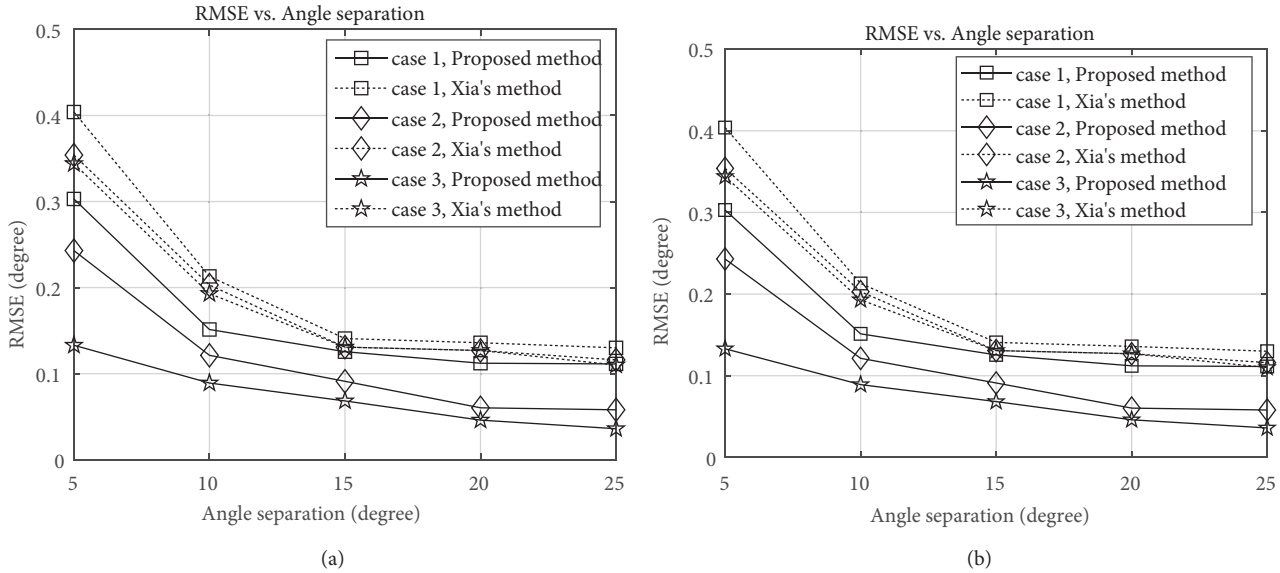

Figure 3. RMSE versus angle separation with snapshots at 1200 and at SNR = 20 dB: (a) θ (b) φ.

4.3. RMSE performance against snapshots

In this simulation, the performance is studied considering different numbers of snapshots varying from 100 to 800. All the other conditions remain similar as supposed in Subsection 4.1 at fixed SNR = 15 dB. Again, it can be concluded that the performance of the proposed method increases as the number of snapshots starts increasing, as shown in Figures 4a and 4b. Moreover, the proposed method outperforms Xia's method in all scenarios, which shows the effectiveness of the proposed method. Our method not only outperform Xia's method in all cases but also outperforms case I and case II itself, which shows the effectiveness of the proposed method when we use a greater number of noncircular sources.

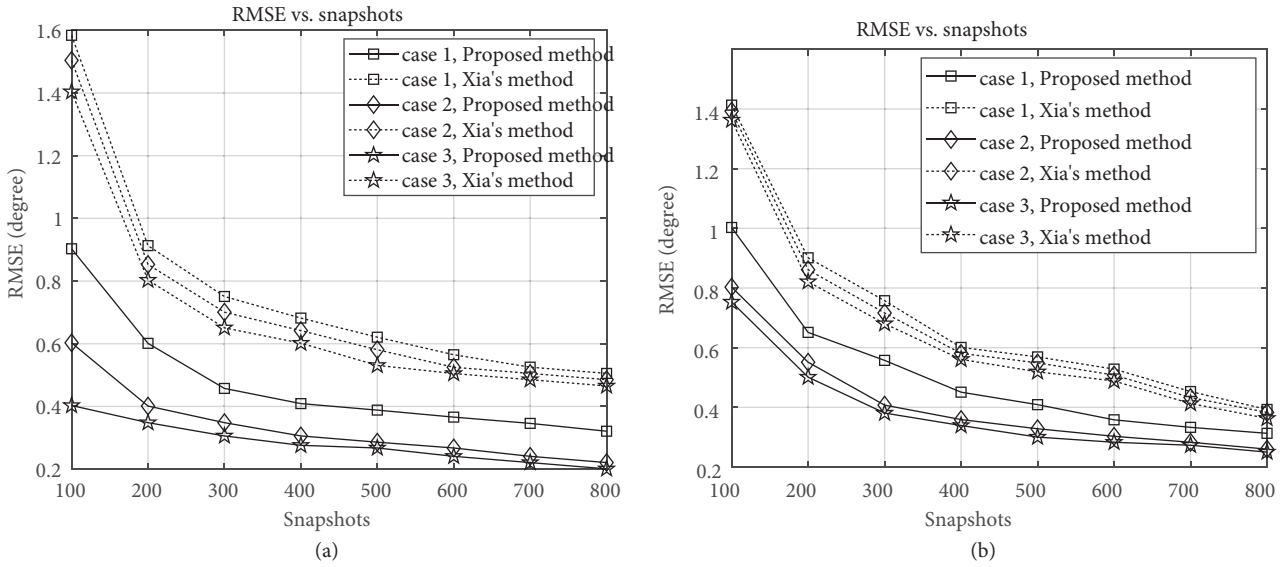

Figure 4. RMSE versus snapshots with SNR = 15: (a) θ (b) φ.

4.4. CRB performance against SNR for noncircular sources

In this section, the objective is to compare our proposed method with deterministic CRB considering only strictly noncircular sources, which we call case IV. All the simulation parameters remain similar as in Subsection 4.1 except snapshots and the total number of sensors in Liu's method is also equal to our proposed method. The RMSE performance is shown in Figures 5a and 5b against SNR from –5 dB to 20 dB. The figure shows that our results are in accordance with the analysis mentioned in [22]. One of the interesting features of our method's case IV is that the RMSE performance of our method exactly became like that of Liu's method, because in this case all sources are noncircular sources and so our performance is similar. However, our method's performance is better than that of Xia's method.

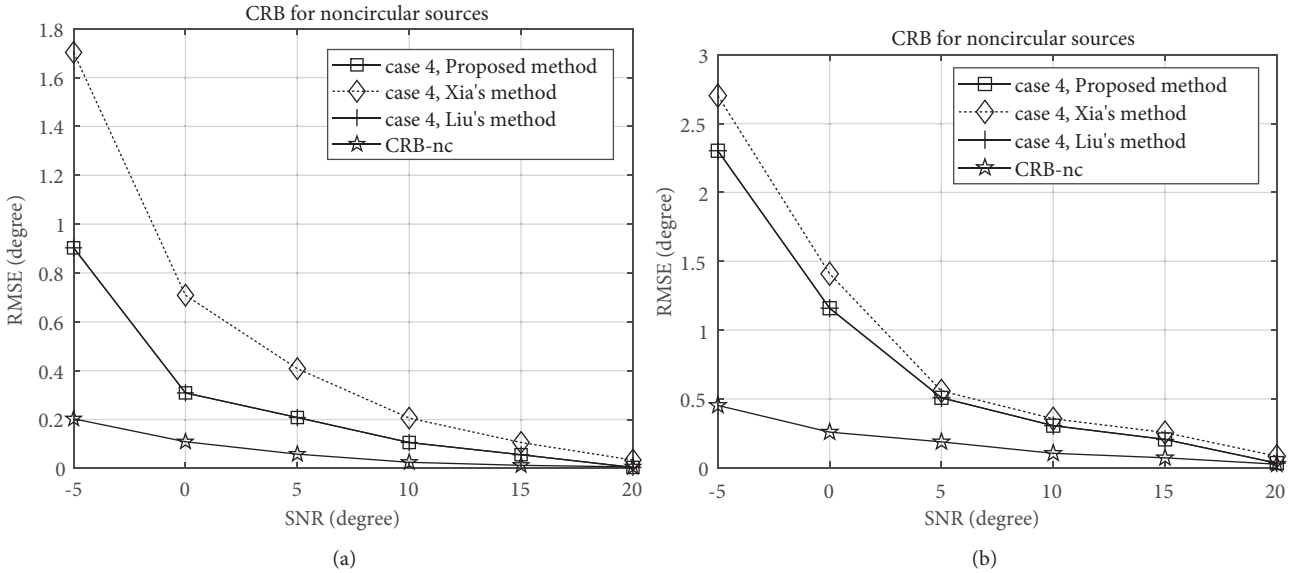

Figure 5. RMSE of CRB versus SNR at snapshots = 1200: (a) θ (b) φ.

5. Conclusion

A novel RARE-based 2-D DOA estimation algorithm has been proposed for a mixture of circular and strictly noncircular sources considering three parallel ULAs. The distinctive steering vectors have been designed to estimate both sources separately. Then RARE-based estimators have been proposed to reduce the computational complexity dramatically by converting 2-D search space into two 1-D search spaces subsequently. The algorithm has some distinctive advantages as it can utilize and can enhance the array aperture efficiently, can estimate greater numbers of sources than sensors, and can provide more accurate estimation as compared to previously proposed methods and additionally there is no need to pair 2-D DOAs as this algorithm can automatically pair 2-D DOAs without any additional complexity and therefore enjoys lower computational complexity.

Acknowledgments

This work was supported by the CAS-TWAS fellowship, the National Natural Science Foundation of China under grant 61671418, and the Advanced Research Fund of the University of Science and Technology of China.

References

[1] Schmidt RO. Multiple emitter location and signal parameter estimation. IEEE T Ant Prop 1886; 34: 276-280.

[2] Krim H, Viberg M. Two decades of array signal processing research: the parametric approach. IEEE Sig Proc Mag 1986; 13: 67-94.

[3] Roy R, Kailath T. ESPRIT-estimation of signal parameters via rotational invariance techniques. IEEE T Acous Spe Sig Proc 1989; 37: 984-995.

[4] Han FM, Zhang XD. An ESPRIT-like algorithm for coherent DOA estimation. IEEE Ant Wir Prop Lett 2005; 4: 443-446.

[5] Pesavento M, Gershman AB, Haardt M. A theoretical and experimental performance study of a root-MUSIC algorithm based on a real-valued Eigen decomposition. IEEE T Sig Proc 2000; 48: 1306-1314.

[6] Zhang Y, Ng BP. MUSIC-like DOA estimation without estimating the number of sources. IEEE T Sig Proc 2010; 58: 1668-1676.

[7] Abeida H, Delmas JP. MUSIC-like estimation of direction of arrival for noncircular sources. IEEE T Sig Proc 2006; 54: 2678-2690.

[8] Xia T, Zheng Y, Wan Q, Wang X. Decoupled estimation of 2-D angles of arrival using two parallel uniform linear arrays. IEEE T Ant Prop 2007; 55: 2627-2632.

[9] Wang G, Xin J, Zheng N, Sano A. Computationally efficient subspace-based method for two-dimensional direction estimation with L-shaped array. IEEE T Sig Proc 2011; 59: 3197-3212.

[10] Chen FJ, Kwong S, Kok CW. Esprit-like two-dimensional DOA estimation for coherent signals. IEEE T Aero Ele Sys 2010; 46: 1477-1484.

[11] Steinwandt J, Roemer F, Haardt M, Del Galdo G. R-dimensional esprit-type algorithms for strictly second-order noncircular sources and their performance analysis. IEEE T Sig Proc 2014; 62: 4824-4838.

[12] Charge P, Wang Y, Saillard J. A noncircular sources direction finding method using polynomial rooting. Sig Proc 2001; 81: 1765-1770.

[13] Gan L, Gu JF, Wei P. Estimation of 2-D DOA for noncircular sources using simultaneous SVD technique. IEEE Ant Wire Prop Lett 2008; 7: 385-388.

[14] Liang J, Liu D. Joint elevation and azimuth direction finding using L-shaped array. IEEE T Ant Prop 2010; 58: 2136-2141.

[15] Gao F, Nallanathan A, Wang Y. Improved MUSIC under the coexistence of both circular and noncircular sources. IEEE T Sig Proc 2008; 56: 3033-3038.

[16] Chen H, Hou C, Zhu WP, Liu W, Dong YY, Peng Z, Wang Q. ESPRIT-like two-dimensional direction finding for mixed circular and strictly noncircular sources based on joint diagonalization. Sig Proc 2017; 141: 48-56.

[17] Zhang Y, Xu X, Sheikh YA, Ye Z. A rank-reduction based 2-D DOA estimation algorithm for three parallel uniform linear arrays. Sig Proc 2016; 120: 1765-1770.

[18] Liu A, Liao G, Xu Q, Zeng C. A circularity-based DOA estimation method under coexistence of noncircular and circular signals. In: IEEE International Conference on Acoustics, Speech, and Signal Processing; 2012. pp. 2561-2564.

[19] Liu ZM, Huang ZT, Zhou YY, Liu J. Direction-of-arrival estimation of noncircular signals via sparse representation. IEEE T Aero Elec Sys 2012; 48: 2690-2698.

[20] Pesavento M, Gershman AB, Wong KM. Direction finding in partly calibrated sensor arrays composed of multiple subarrays. IEEE T Sig Process 2002; 50: 2103-2115.

[21] Liu J, Huang ZT, Zhou YY. Azimuth and elevation estimation for noncircular signals. Electron Lett 2007; 43: 1117-1119.

[22] Roemer F, Haardt M. Efficient 1-D and 2-D DOA estimation for non-circular sources with hexagonal shaped ESPAR arrays. In: IEEE International Conference on Acoustics, Speech, and Signal Processing; 2006. pp. 1-4.

Appendix

Here, the objective is to prove that Eqs. (23) and (24) are alike. Examining carefully, the basic difference between the equations is only the difference of noise subspace. Hence, focusing on only noise subspace, our objective is to show that

$$\mathbf{E}_{n1}\ \mathbf{E}_{n1}{}^{H} = \left(\ \mathbf{E}_{n2}\ \mathbf{E}_{n2}{}^{H}\right)^{*}. \tag{34}$$

Proof: $\mathbf{E}_n$ can be partitioned into two equal submatrices $\mathbf{E}_n$. Therefore,

$$\mathbf{P} = \ \mathbf{E}_n\ \mathbf{E}_n{}^{H} = \ \mathbf{E}_n\ \mathbf{E}_n{}^{H}, \tag{35}$$

$$\mathbf{E}_n\ \mathbf{E}_n{}^{H} = \begin{bmatrix} \mathbf{E}_{n1} \\ \mathbf{E}_{n2} \end{bmatrix} \begin{bmatrix} \ \mathbf{E}_{n1}{}^{H} & \mathbf{E}_{n2}{}^{H}\ \end{bmatrix}, \tag{36}$$

$$= \begin{bmatrix} \mathbf{E}_{n1}\ \mathbf{E}_{n1}{}^{H} & \mathbf{E}_{n1}\ \mathbf{E}_{n2}{}^{H} \\ \mathbf{E}_{n2}\ \mathbf{E}_{n1}{}^{H} & \mathbf{E}_{n2}\ \mathbf{E}_{n2}{}^{H} \end{bmatrix}. \tag{37}$$

Taking the conjugate on both sides,

$$\mathbf{E}_n\ \mathbf{E}_n{}^{H} = \begin{bmatrix} \mathbf{E}_{n2}{}^{*} \\ \mathbf{E}_{n1}{}^{*} \end{bmatrix} \begin{bmatrix} \ \mathbf{E}_{n2}{}^{T} & \mathbf{E}_{n1}{}^{T}\ \end{bmatrix} \tag{38}$$

$$= \begin{bmatrix} \mathbf{E}_{n2}{}^{*}\ \mathbf{E}_{n2}{}^{T} & \mathbf{E}_{n2}{}^{*}\ \mathbf{E}_{n1}{}^{T} \\ \mathbf{E}_{n1}{}^{*}\ \mathbf{E}_{n2}{}^{T} & \mathbf{E}_{n1}{}^{*}\ \mathbf{E}_{n1}{}^{T} \end{bmatrix} = \begin{bmatrix} \left(\ \mathbf{E}_{n2}\ \mathbf{E}_{n2}{}^{H}\right)^{*} & \left(\ \mathbf{E}_{n1}\ \mathbf{E}_{n2}{}^{H}\right)^{*} \\ \left(\ \mathbf{E}_{n1}\ \mathbf{E}_{n1}{}^{H}\right)^{*} & \left(\ \mathbf{E}_{n1}\ \mathbf{E}_{n1}{}^{H}\right)^{*} \end{bmatrix}. \tag{39}$$

Therefore, comparing Eqs. (37) and (39),

$$\mathbf{E}_{n1}\ \mathbf{E}_{n1}{}^{H} = \left(\ \mathbf{E}_{n2}\ \mathbf{E}_{n2}{}^{H}\right)^{*}, \tag{40}$$

and using Eq. (35) it can be simply written:

$$\mathbf{E}_{n1}\ \mathbf{E}_{n1}{}^{H} = \left(\ \mathbf{E}_{n2}\ \mathbf{E}_{n2}{}^{H}\right)^{*}. \tag{41}$$

Hence, the proof is completed.